NISTIR 6872

Evaluation of Fire Models for Nuclear Power Plant Applications: Cable Tray Fires

International Panel Report

Compiled by Monideep K. Dey, Guest Researcher

National Institute of Standards and Technology
Technology Administration, U.S. Department of Commerce

NISTIR 6872

Evaluation of Fire Models for Nuclear Power Plant Applications: Cable Tray Fires

International Panel Report

Compiled by Monideep K. Dey, Guest Researcher
Fire Research Division
Building and Fire Research Laboratory

June 2002

U.S. DEPARTMENT OF COMMERCE
Donald L. Evans, Secretary
TECHNOLOGY ADMINISTRATION
Phillip J. Bond, Under Secretary of Commerce for Technology
NATIONAL INSTITUTE OF STANDARDS AND TECHNOLOGY
Arden L. Bement, Jr., Director

Appendix D: Benchmark Analysis with CFX, Matthias HEITSCH, GRS, Germany

Gesellschaft für Anlagen-
und Reaktorsicherheit
(GRS) mbH

CFX Simulations for the Benchmark Exercise #1
- Cable Tray Fires of Redundant Safety Trains -

International Collaborative Project to Evaluate Fire Models
for Nuclear Power Plant Applications

Dr. Matthias Heitsch

Technical Note HET 1/2001

Gesellschaft für Anlagen- und Reaktorsicherheit (GRS) mbH
Schwertnergasse 1
D-50667 Koeln
Tel: +49 221 2068 678
Fax: +49 221 2068 834
Email: het@grs.de

Content

List of Figures and Tables

Abbreviations

CFD	Computational Fluid Dynamics
NPP	Nuclear Power Plant

1 Introduction

A benchmark exercise has been set up to evaluate the capabilities of codes to model relevant phenomena with cable tray fires in a NPP. According to the specification of this Benchmark Exercise part 1 [DEF 00] out of the large number of numerical cases specified a representative selection has been simulated by the help of the general-purpose CFD code CFX 4.3. The motivation of the application of CFX has been to find out how it performs in comparison with other probably more specialised codes. It is also of interest under which conditions the specific characteristics of CFX are beneficial and can justify the higher computing costs. So far, due to restrictions in the computing resources available not the complete suite of specified test cases has been simulated. However, the presented selection is believed to provide a good idea of the capabilities when applying CFX. Work will be continued based on the experience got from the meeting in Palo Alto in January 2001.

2 The CFD Code CFX

The code CFX-4.3 [AEA 99] provides numerical approximations of the Navier-Stokes equations on a finite volume basis. The program version applied here uses a block-structured grid with body fitted coordinates. Block-structured means that all blocks of the computational domain have to be designed with a hexahedral shape. With complex geometries this implies occasionally finer grids than really necessary.

The code offers a number of physical models to simulate a wide range of flow problems. Among these are:

- Arbitrary multi-component mixtures,
- Turbulence models for low and high Reynolds numbers,
- Multi-phase models including a versatile multi-fluid model and a homogeneous two-phase model,
- Particle transport model,
- Complex thermal radiation model based on a Monte-Carlo formulation,

- Chemical reaction capability,
- Convective heat transfer and heat conduction,
- User Interface to modify existing or add own models.

The given benchmark makes use of the turbulence (k-ε) and multi-component models combined with the thermal radiation package. Chemical reactions, although possible, are not included in the simulations so far.

3 Analyses on Part 1

In part 1 of the benchmark exercise a trash bag fire in the vicinity of a cable tray inside an emergency switchgear room (Fig. 1) is to be simulated. The objective "is to determine the maximum horizontal distance between a specified transient fire from the trash bag and tray A (Fig. 1) that results in ignition of tray A" [DEF 00]. For simplicity the cable tray represented by a single power cable of 50 mm. The room has ventilation and a fire proof door. A base case and five related simulations with variations of the distance between cable tray and fire, the door open or closed and the ventilation system on or off are to be investigated. The time to be covered is 600 s. The total heat release from the trash bag is specified in Fig. 3 and the radiative fraction is fixed to be 30%. This specification implies not to simulate the chemical reactions in the trash bag explicitly rather than using the heat release curve and study the convective and radiative flows induced by the fire in the trash bag.

A computer model was developed which is composed of 28400 fluid cells (Fig. 2). The grid resolution could be refined easily but is left on this rather crude level to comply with the number of test cases and the problem time of this exercise. The model contains the trash bag and the target cable (representing tray A) inside the room. In order to save computing time the outer walls are not modeled. This results in an overestimation of the heat losses from the fire room atmosphere because the heat up of inner wall sections is neglected and consequently the temperature difference gas to wall is too large. The given convective heat transfer coefficient of 15 W/m^2K is applied. For some of the cases the openings of the ventilation system and the fire door can be opened. In all other cases a crack of specified size around the door is available.

There are several options to implement the heat release from the trash bag. Currently the trash bag is modeled as a solid body with the convective fire heat release from the nearest cells around it and with radiation from its surface. The trash bag could also be a hollow body with the convective heat released from all the internal cells. Because radiation can only be emitted from a surface, in this case the top surface could be used for the radiation source. The benchmark specification does not further localize the heat sources therefore the first option has been implemented. During the simulations it turned out that the shape of the trash bag fire changed from time to time. However if numerical reasons or inherent instabilities cause this behavior has not been further investigated.

Conduction in the target cable is included. The cable itself is represented as a cylinder of appropriate size and can be moved within the grid according to the different test cases.

The atmosphere within the fire room is assumed to be air. Individual gas species are not modeled because the fire chemistry is not included.

3.1 Base Case

In the base case the target cable has a horizontal distance of 2.2 m from the trash bag. The door is closed and the ventilation system is off. It is the first case simulated and is discussed in more detail. The moment of the highest heat release from the trash bag is depicted in Fig. 4. The plume around the trash bag and the induced upwards directed flow is influenced by the option of the heat release chosen and may be different if modeled by the other option (see chapter 3). The target cable is affected by a flow directed downwards as indicated in Fig. 4. At the moment of strongest heat release the warmer gas is concentrated below the ceiling of the room as shown in Fig. 5. Some flow is directed towards the crack in the fire door. After 600 s the temperature distribution in the room is shown in Fig. 6. At this time gas temperatures do not show a remarkable stratification. Close to the walls temperatures are lower due to the heat losses resulting from the high heat transfer coefficient given. This behavior is illustrated in Fig. 7. From bottom to top the temperature does not vary much. Underneath the ceiling it increases considerably (buoyant flow) before wall cooling is dominating. With a higher gas temperature the heat flux to the wall increases and provokes a higher temperature gradient compared with the bottom region. From the temperature profile in Fig. 7 a subdivision

of the room into a hot layer above a cold layer appears to be inadequate. Of interest is the distribution of heat flows to walls and target cable. All flows reach their maximum at the time with the highest heat release. The total heat flux to the cable in comparison with the flow to the walls (Fig. 8) is less than the surface ratio. This may be due to the lower wall temperatures. In Fig. 8 decreases the radiative fraction to the cable to a very small value when the fire heat release decreases after its maximum. The hotter cable then loses energy to the cooler walls. The heat captured by the cable does not lead to a measurable increase of the centerline temperature. The surface temperature develops as shown in Fig. 9 and has almost no further increase after the maximum heat flow from the trash bag is passed.

3.2 Case 1

Case 1 differs from the base case only by another location of the trash bag relative to the target cable. The trash bag is directly below the target cable. The moment of maximum heat release is depicted in Fig. 10. Compared with the base case the cable is now completely inside the hot gas stream from the fire. This results in a higher heat-up of the cable surface as shown in Fig. 12. The maximum is now about 550 K. In the base case it was only 360 K. After the maximum heat is passed the surface temperature goes down as well. The power to the cable over time shown in Fig. 11 has a maximum of about 700 W. This is considerably more than in the base case with 500 W. Another difference is the radiative behavior. With this case in the late phase the cable radiates energy to the surroundings and is therefore cooled.

The centerline temperature remains almost unchanged during the simulation time. Other cases with larger distances of the trash bag than the actual will not be able to create higher cable temperatures with a chance of ignition (643 K).

3.3 Case 5

Case 5 is interesting because of the flow patterns influenced by the ventilation system now on. The position of the trash bag is identical to the base case. Compared with the base case the cable is now in a more upwards flow. This is depicted in Fig. 13. Equally, the heat-up of the cable is very similar and remains low (Fig. 14). The ventilation system with a continuous inflow of cold air does not alter things considerably.

Chemical reactions including oxygen consumption have not been modelled. However, an oxygen depletion which might be avoided by the fresh air entering through the ventilation opening is not realistic because of the short simulation time.

A comparison of all three simulated cases in terms of the cable surface temperature is depicted in Fig. 15. With the given ignition criterion only the location of the fire directly below the target cable would have a chance to ignite the cable over a longer time or with a higher heat release.

4 Analyses on Part 2

This part of the benchmark is to “determine the damage time of the target cable tray B for several heat release rates of the tray stack (A,C2, C1), and horizontal distance D. The effects of target elevation and ventilation will also be examined.” [DEF 00]. The duration of the fully developed fire is fixed to be 3600 s (including transitions 4800 s). To perform a reasonable number of simulations in a short time the computational grid was set to have less cells than for part 1. It is shown in Fig. 16. The model now has 11400 cells. This includes the cells to represent the solids of the cable trays and the target cable (instrumentation cable of 18 or 50 mm diameter). The simulated fire heat from the trays A, C1, C2, which are lumped together, follows the shape shown in Fig. 18. The peak can be between 1 and 3 MW. The target cable is considered to be damaged when the centerline of the cable reaches 200 C.

The release of the heat from the assumed fire is implemented similarly to part 1. The convective fraction is placed as volumetric source into the cells closest to the cable trays. The radiative fraction of 48% is emitted directly from the solid surfaces.

With the longer simulation time the heat absorbed by the boundary walls and the subsequent rise of the surface temperature should not be neglected. Therefore a one dimensional heat conduction simulation has been added. Compared with an explicit inclusion of the walls (this means by conducting cells) the computing time is negligible.

Chemical reactions are not treated in the simulations. Hence no check for oxygen depletion has been done in the code. Only a crude hand approximation has been done. From the specifications it remains unclear how to proceed with the fire heat release if oxygen depletes for a time but then recovers by the ventilation system.

4.1 Base Case

This case is distinguished from other cases by a peak heat release rate of 1 MW and a distance of the power cable (diameter 50 mm) of 6.1 m. The door is closed and the ventilation system is off.

With the higher heat release and all openings closed it is likely that the available oxygen is exhausted soon. An approximation indicates a time of about 1200 s. This time has been selected for the illustration in Fig. 17. A global circulation can be observed and the temperature is rather uniform.

It is speculative how the case would further develop if oxygen depletes because this is not modeled currently. To be conservative the simulation over the full time and the heat release according to Fig. 18 has been performed.

The heat flow to the cable which is at the same elevation like the burning cable trays leads to a rapid heat up of its surface (Fig. 19). Therefore radiation from the cable to the colder boundary walls is positive which means that the cable loses energy. Consequently the heat-up of the cable is reduced. A look to the cable temperatures gives Fig. 20. Although at the surface very soon high values are reached, in the central part of the cable only about 50 K increase is obtained. Therefore no damage with the given criterion can be detected. This is true either after 1200 s when the available oxygen tends to deplete or after 4800 s when following the given heat release curve to full extent.

4.2 Case 6

The base case is only capable of producing a relatively low heat-up of the target. Among the specified cases case 6 assumes the highest peak heat value (3 MW) in combination with the nearest placement of the target cable to the fire source. With higher heat output from the fire oxygen will deplete earlier. According to an approximation this may be after 700 s. After this time the flow field and temperature distribution calculated by CFX is shown in Fig. 21. A large vortex has developed with a horizontal flow along the floor. Fig. 23 compares the temperature in the center of the room of case 6 with the base case. For both cases simulations have been extended beyond the oxygen depletion point up to the end of the specified fire duration. Case 6 leads to a much higher room temperature. However the early oxygen starvation prevents a target

damage. The centerline temperature reaches values above the damage threshold of 423 K only in the late phase of the simulation. This is shown in Fig. 22. A summary of the heat flows received by walls and the target is illustrated in Fig. 24. Right from the beginning the target becomes that hot that it constantly loses energy to the outer walls. However, by gas convection it is heated further.

4.3 Case 10

Both cases analysed up to now suffer from early oxygen starvation although the fire power might be strong enough to damage the target cable. A fresh air flow through the room might change the situation. Case 10 is comparable with the base case but the door is open and the ventilation system is working. Oxygen depletion has therefore been excluded. The incoming air is cold and forms therefore a stable stratification in the room. Fig. 25 and Fig. 26 illustrate this from different perspectives. The flows out of the door and the ventilation system can be seen. A cooling effect to the target cable is not expected. If oxygen around the burning cable trays is sufficiently available can not be answered unless the migration and distribution of the species involved would be modeled in detail. Under the assumption of abundant oxygen to feed the fire, the cable centerline temperature is calculated as shown in Fig. 27. There is only little heating-up in the center of the cable.

5 Summary

Following the benchmark specification a selection of six cases out of a total of 20 for both parts has been simulated by the CFD code CFX. Despite this reduced number of cases they were selected with the intention to preserve the scope of the benchmark and to get representative results.

The analyses carried out demonstrate the capabilities of CFD codes in simulating fire situations. They also outline the higher effort with respect to computing resources. On a DEC-Alpha Unix machine with about 350 Mflops simulations needed approximately 64 h and 153 h for part 1 (28400 cells) and part 2 (11400 cells), respectively.

In order to keep computing times manageable it was decided to use relatively coarse grids for both parts of the benchmark.

None of the cases analysed leads to a damage of the target cable according to the specified damage criterion for part 1 and 2. This is true if depletion of oxygen is included in the simulations. If these are carried out following the heat release curves to full extent then case 6 leads to cable damage.

6 Continuation of Work

An obvious continuation of the current work is the simulation of other important test cases. Among these are for part 2 case 9 with partial activation of the ventilation system and opening of the door in the room. This will enable to investigate whether oxygen depletion will occur later than in previous cases. A realistic chance of cable damage may involve case 13 with a cable diameter of 15 instead of 50 mm.

It will be necessary to investigate the quality of the grids for both models applied so far. With finer grid cells at around source and target it can be proved if grid convergence with the solutions found has been achieved.

A crucial point for many cases is the depletion of oxygen. To provide realistic simulations mixing and diffusion of oxygen in combination with the consumption of the fire need to be included into the fire model of CFX. This means that for the relevant species additional conservation equations have to be solved.

References

AEA 99 CFX4.3, Documentation, CFX International, AEA Technology plc, Oxfordshire, United Kingdom, 1999.

DEF 00 Benchmark Exercise, Definition of Problem, Revised June 19-20,2000.

Figures and Tables

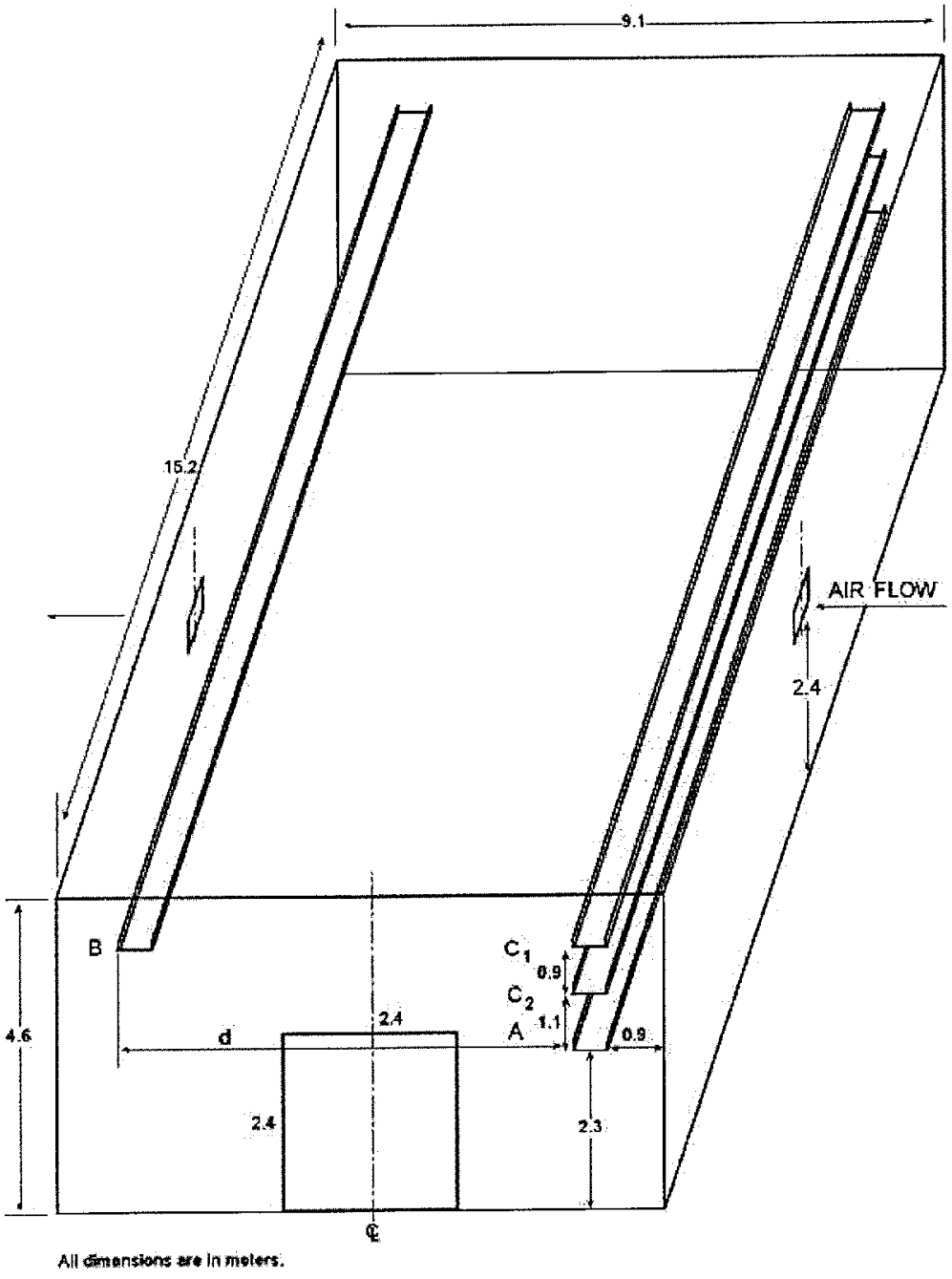

Fig. 1 View of the room to be modeled

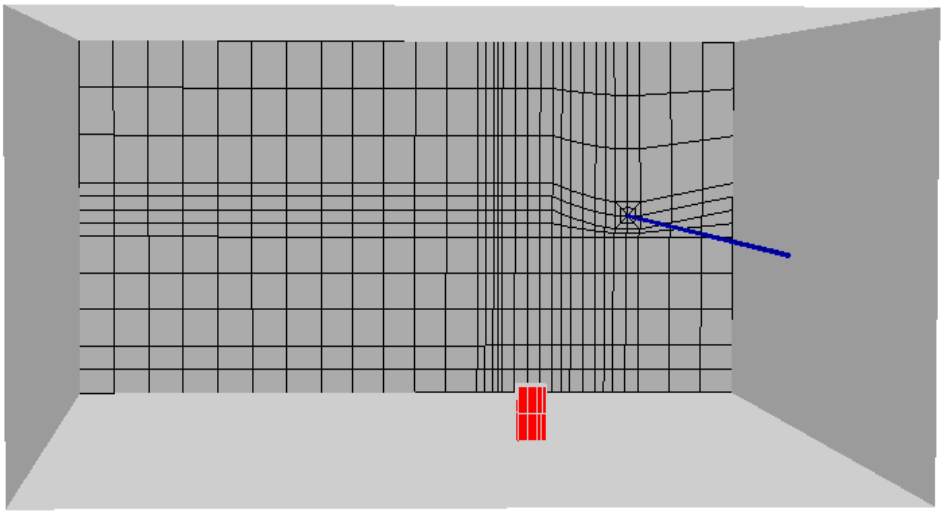

Fig. 2 View of the computer model for part 1

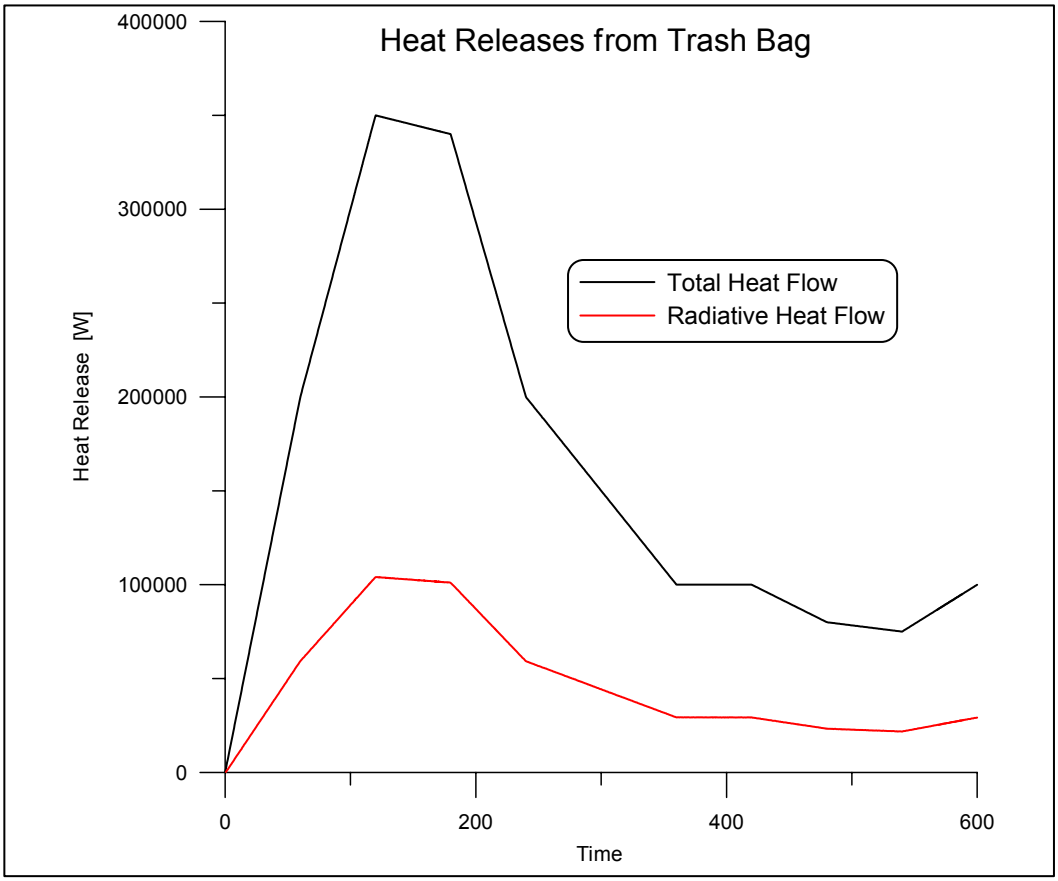

Fig. 3 Overview of given heat release over time (Part 1)

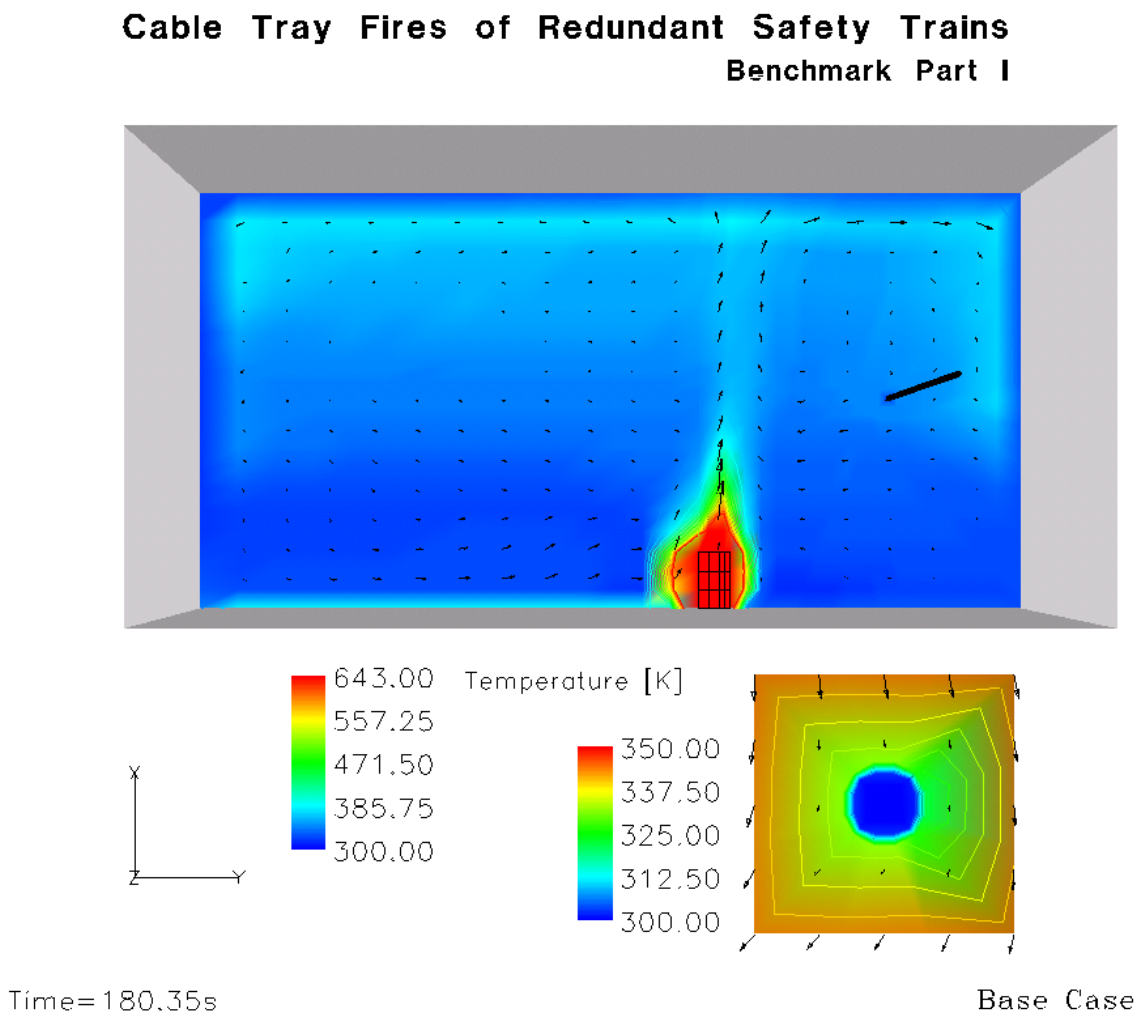

Fig. 4 Temperature distribution at the time of strongest heat release (base case)

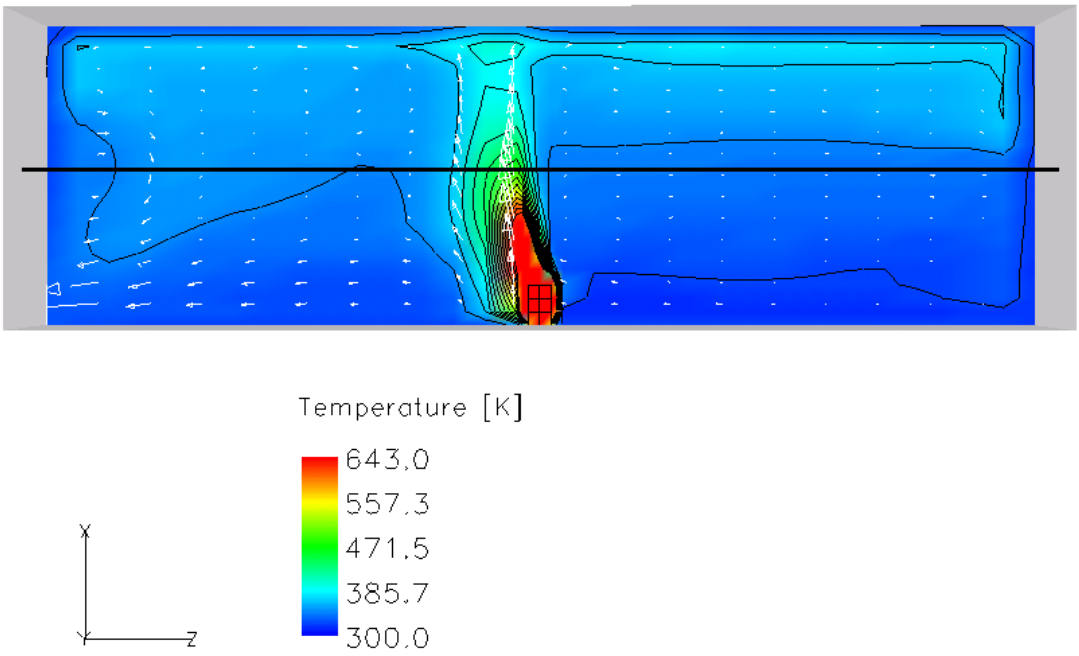

Fig. 5 Lateral view of the fire room after 180 s (base case)

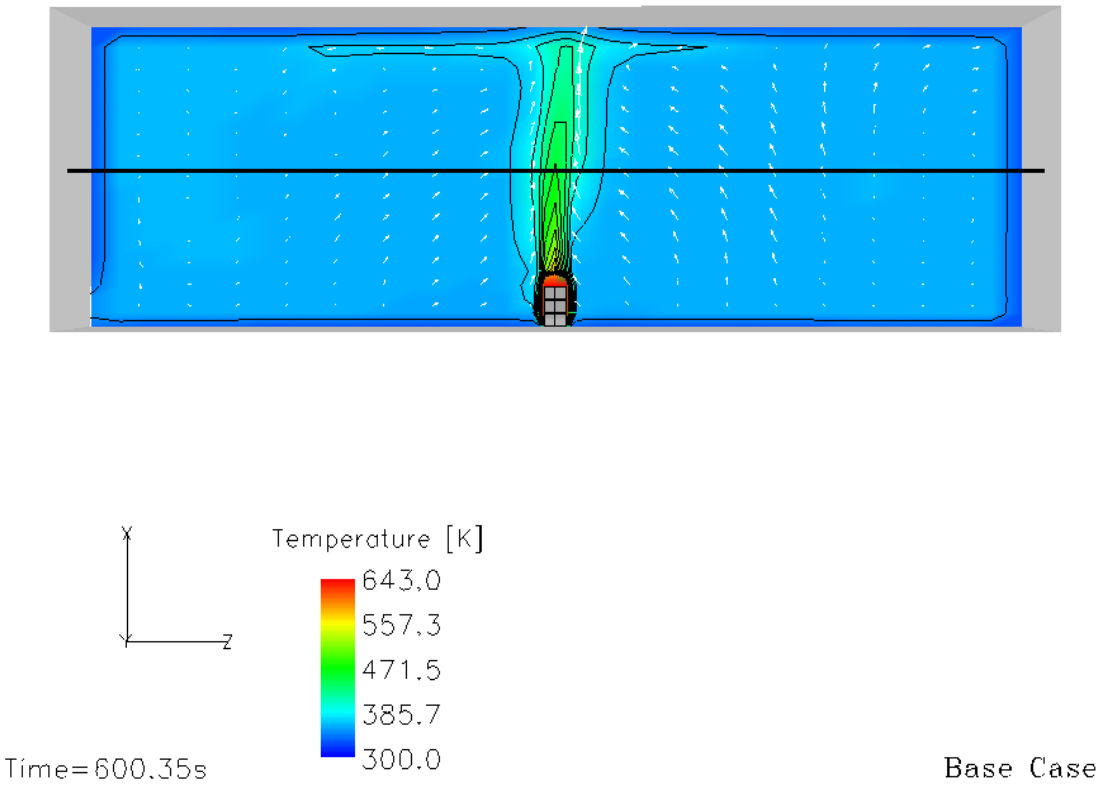

Fig. 6 Temperature distribution after 600 s (base case)

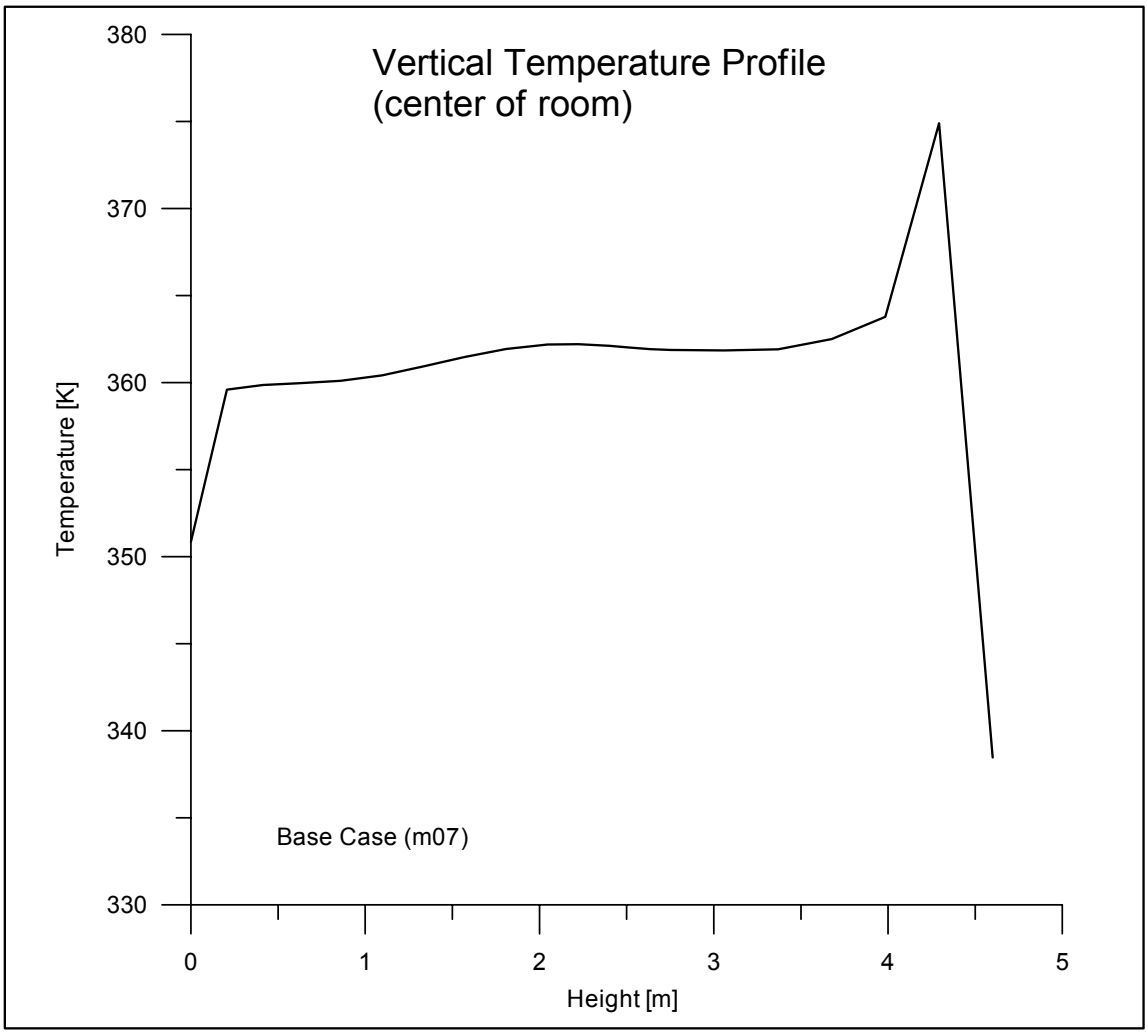

Fig. 7 Vertical temperature profile from bottom to top after 600 s (base case)

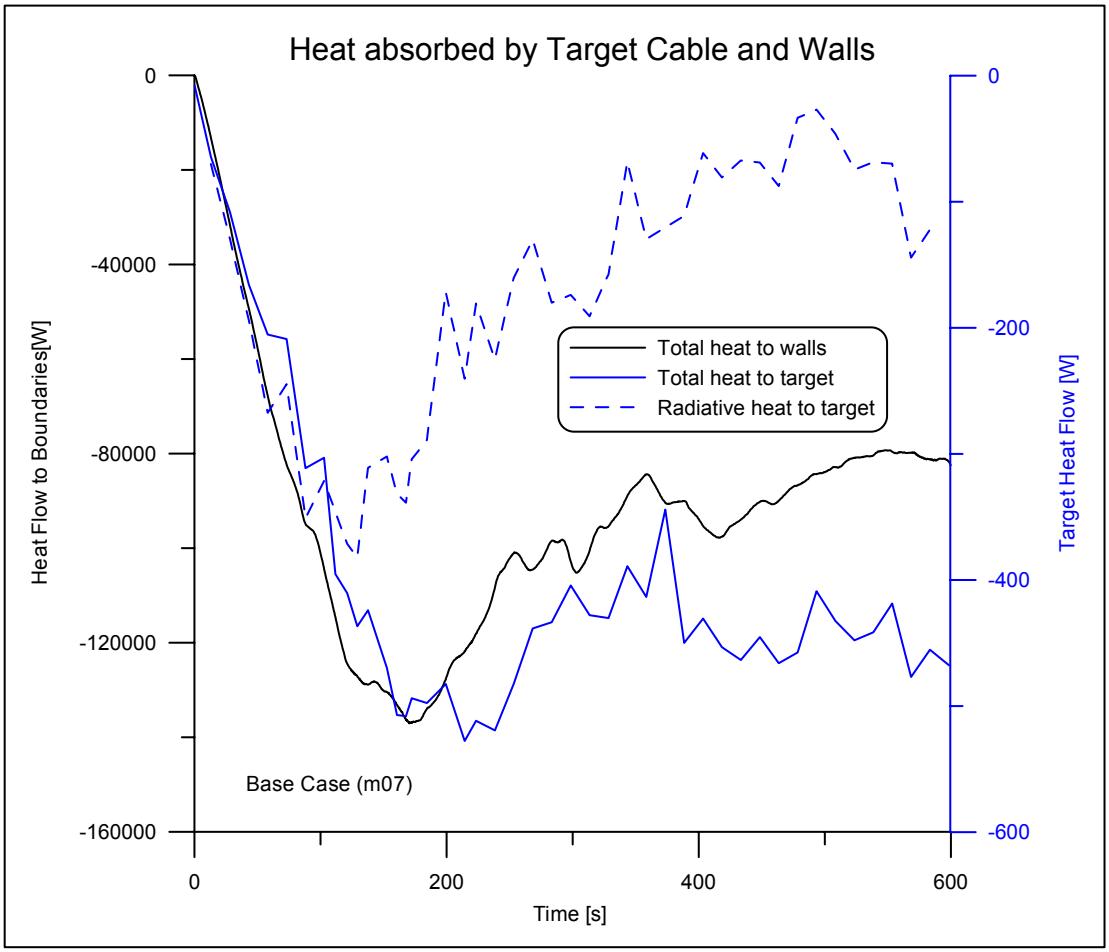

Fig. 8 Heat absorbed by the target cable (base case)

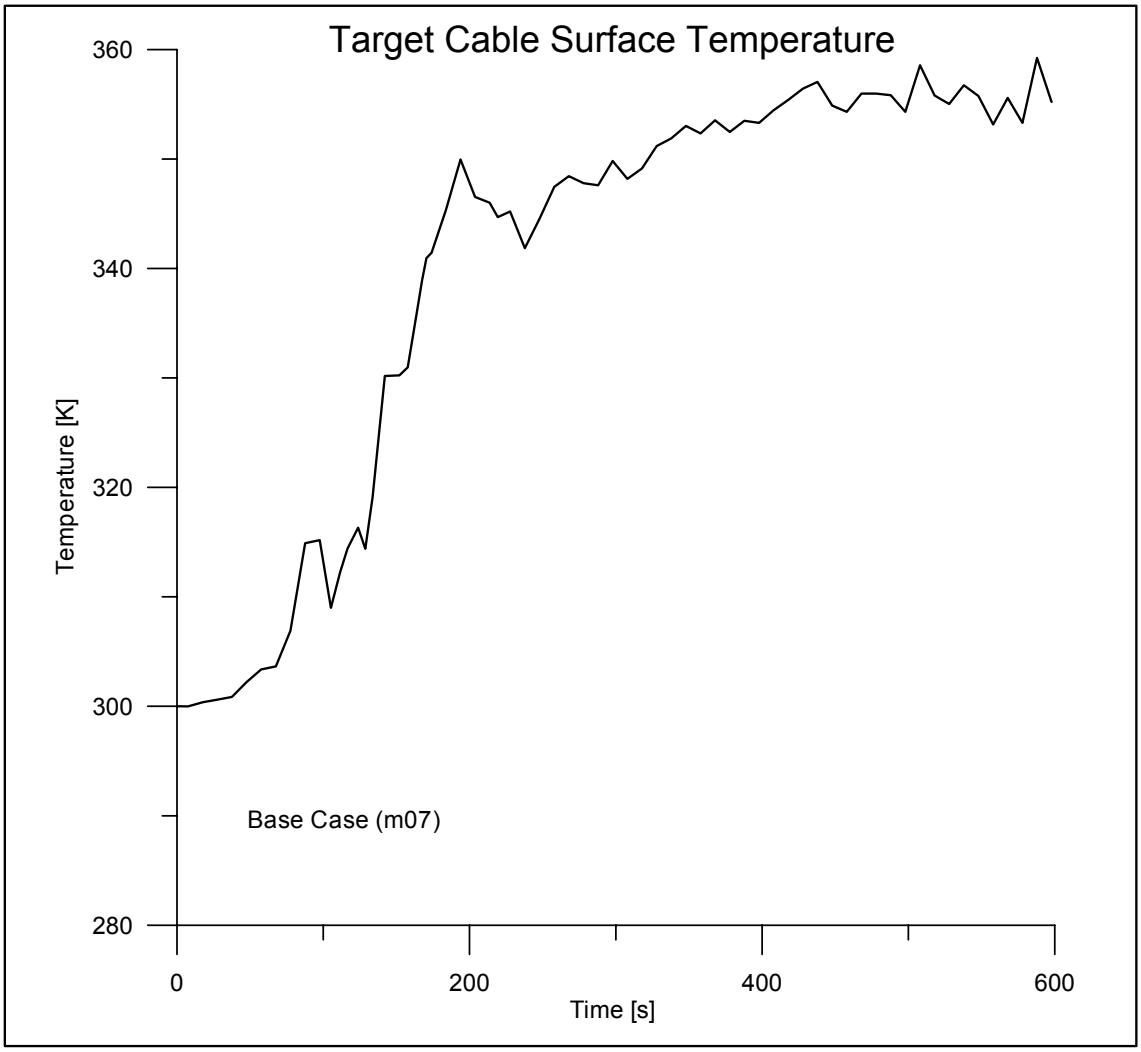

Fig. 9 Target cable surface temperature variation for the base case

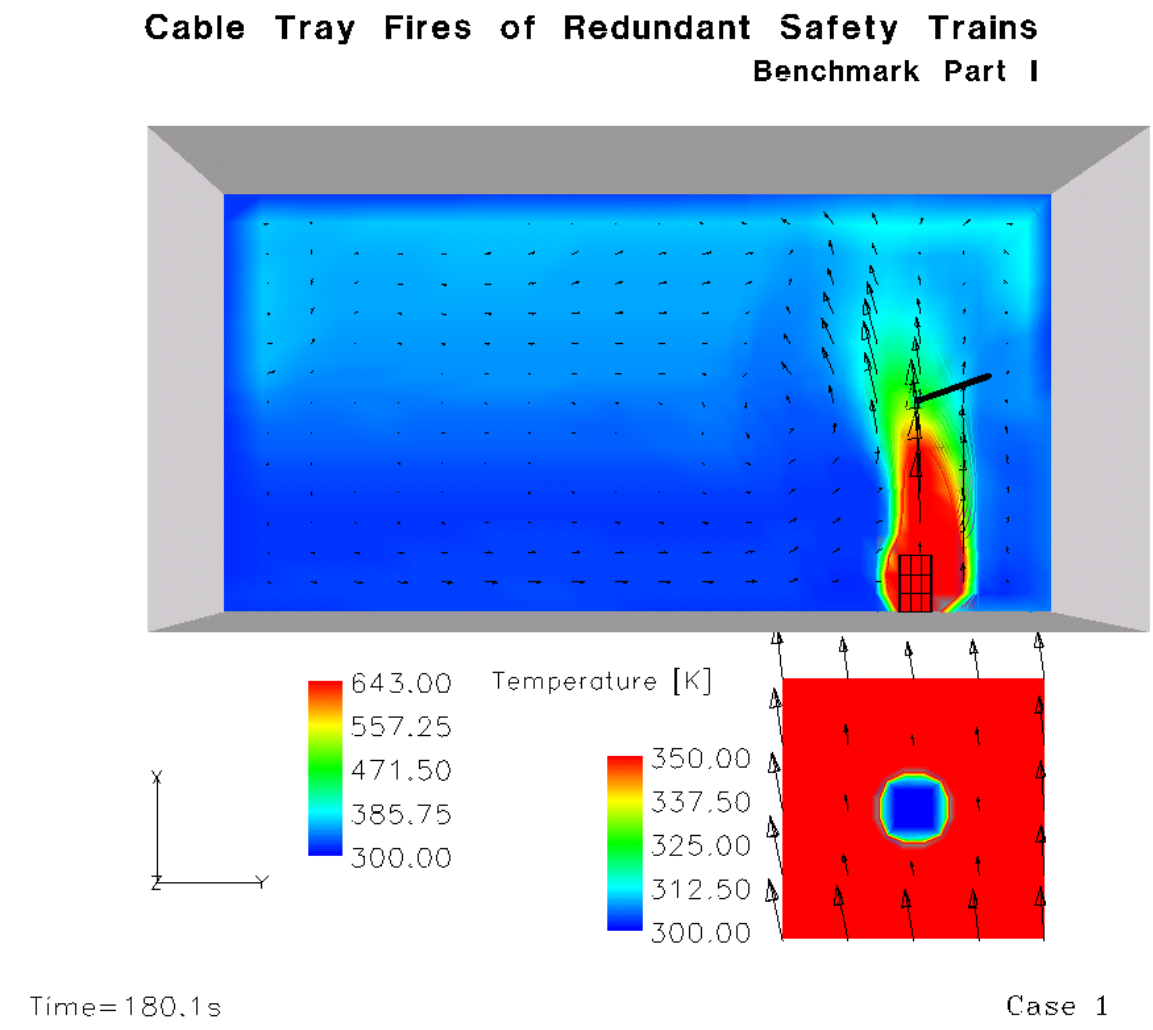

Fig. 10 Flow field and temperature distribution in the room foe case 1

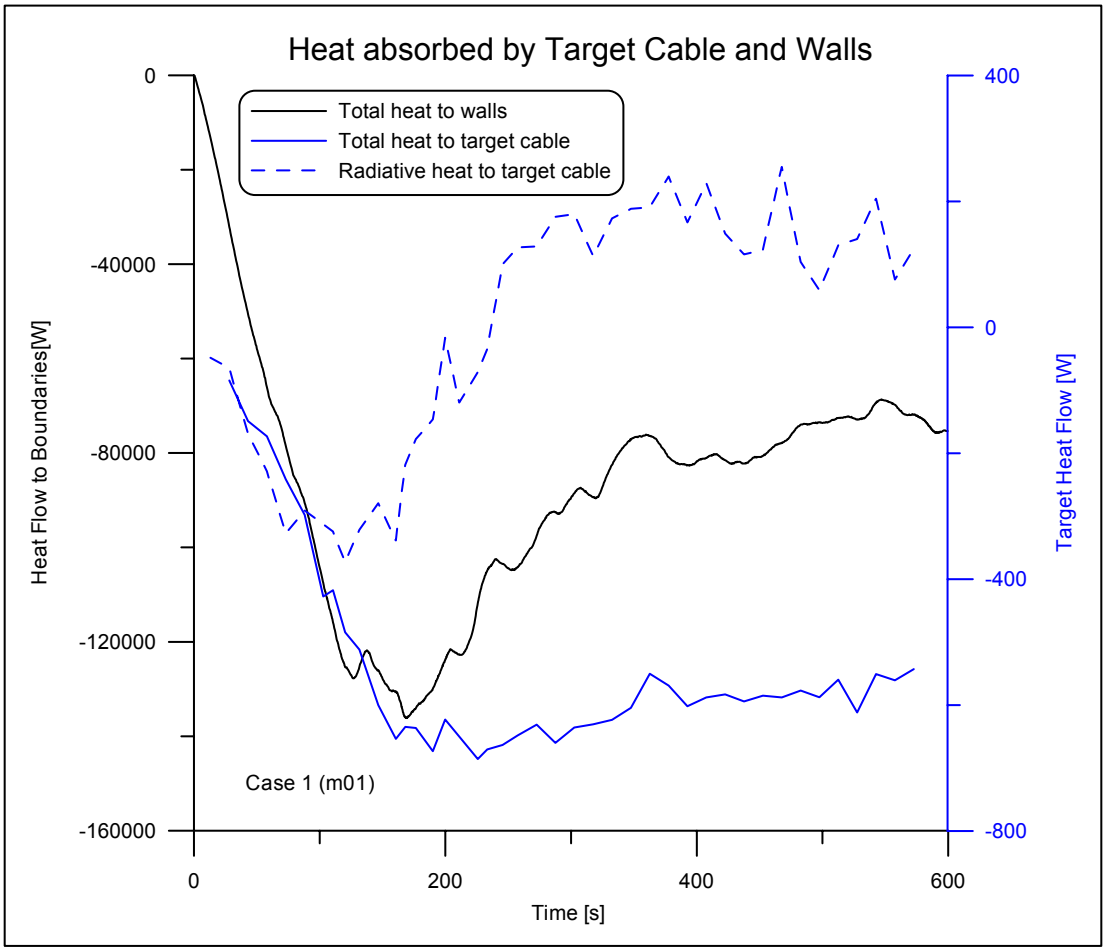

Fig. 11 Heat fluxes for case 1

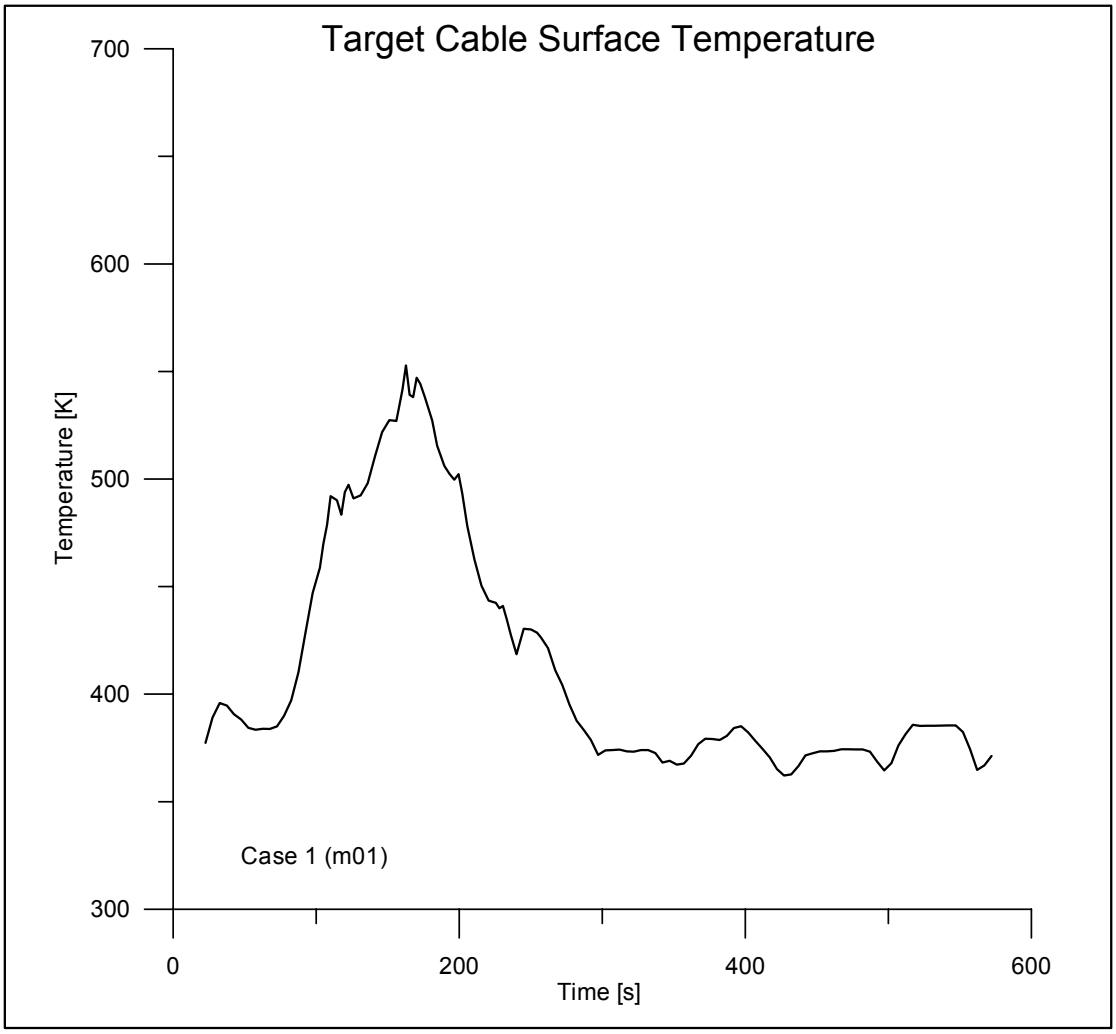

Fig. 12 Surface temperature over time for case 1

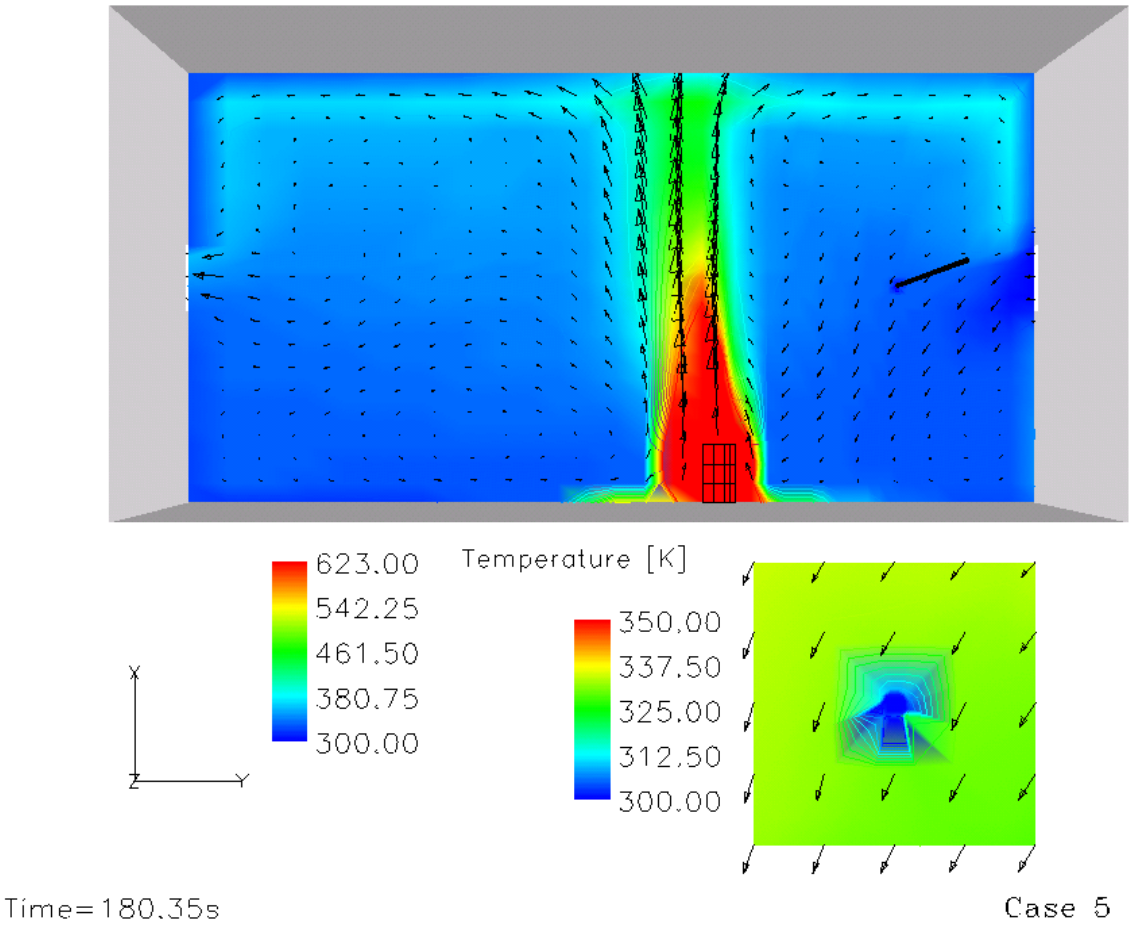

Fig. 13 Flow field in the fire room with ventilation system on (case 5)

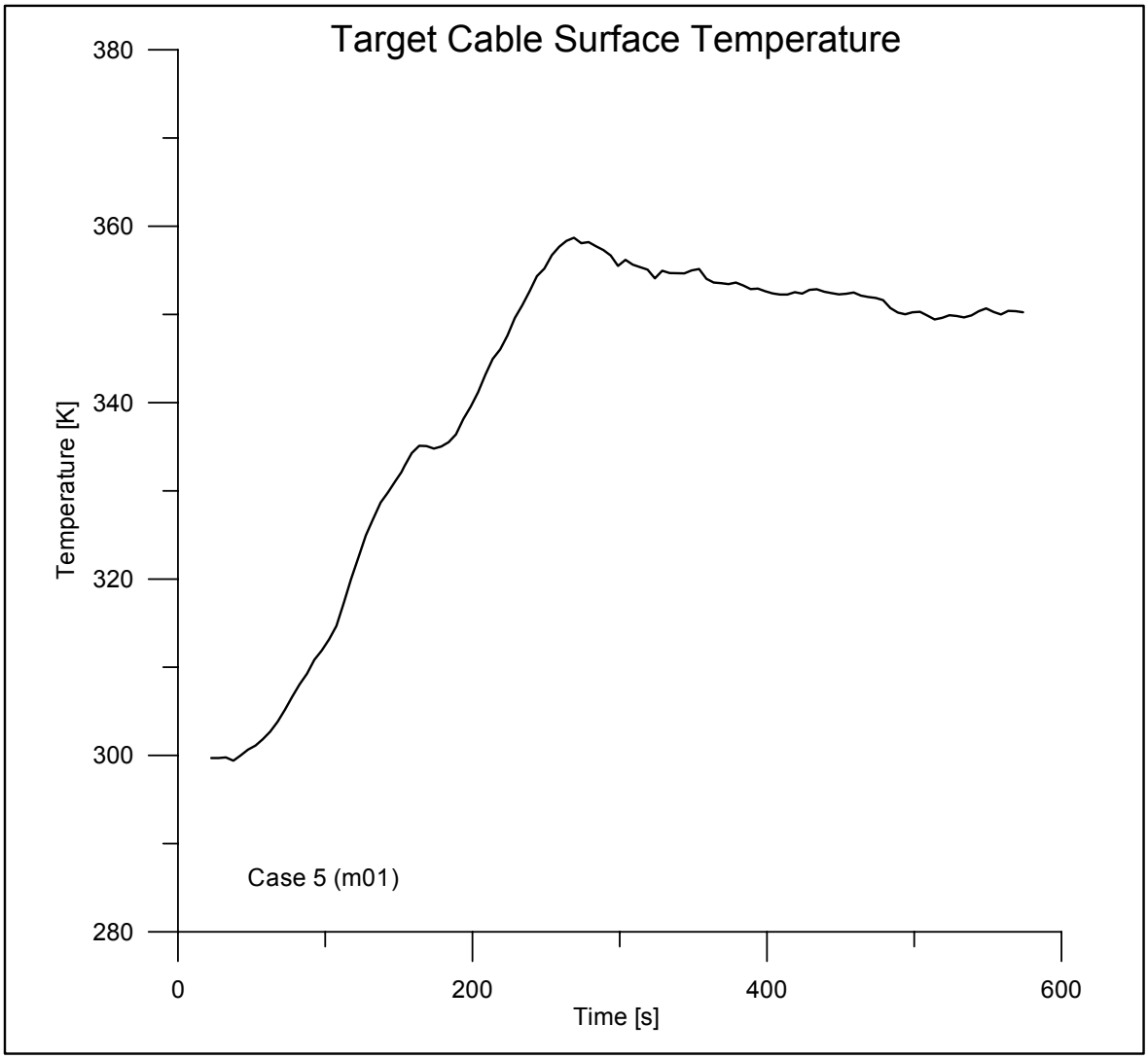

Fig. 14 Cable surface temperature with case 5

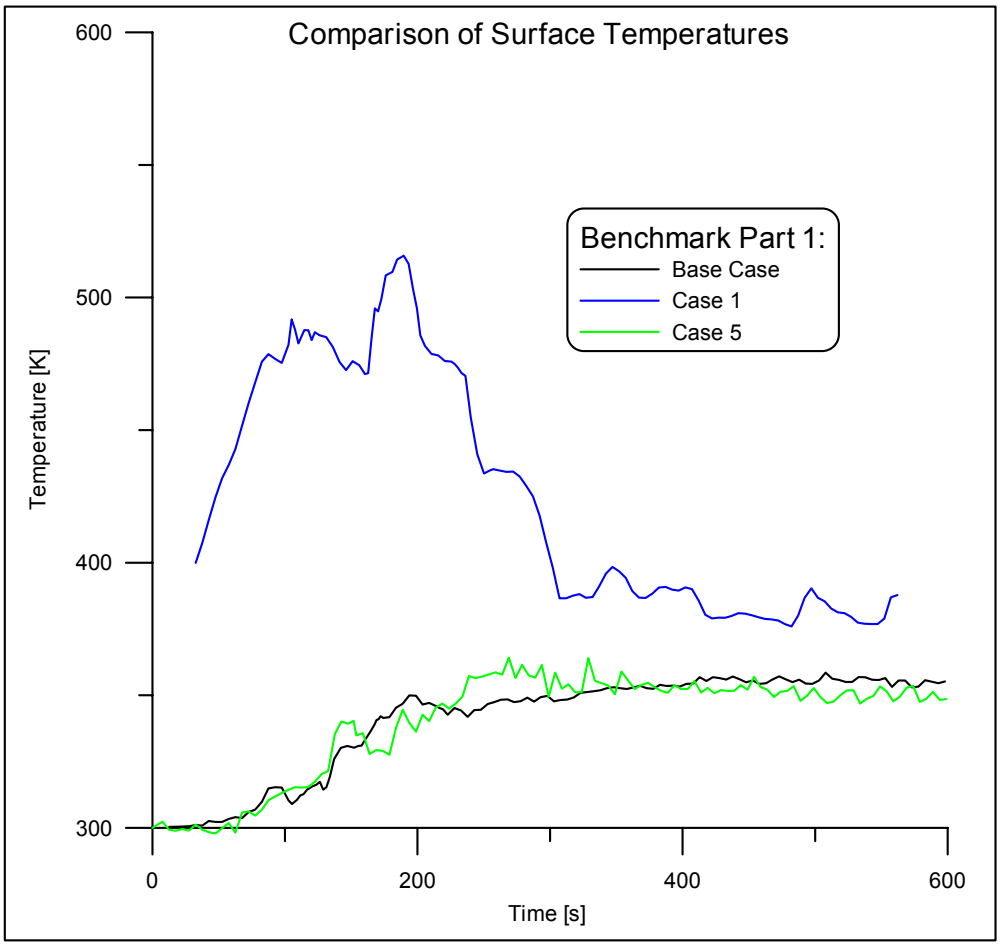

Fig. 15 Comparison of surface temperatures for benchmark part 1

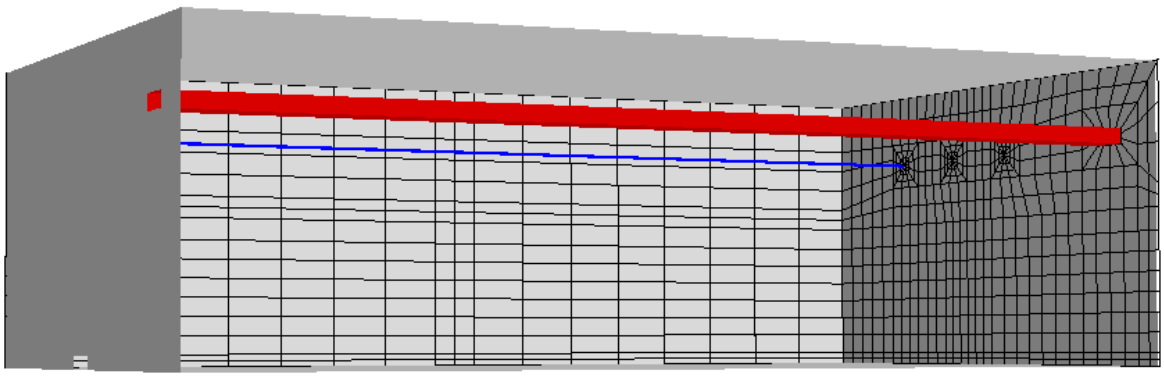

Fig. 16 CFX model for benchmark part 2

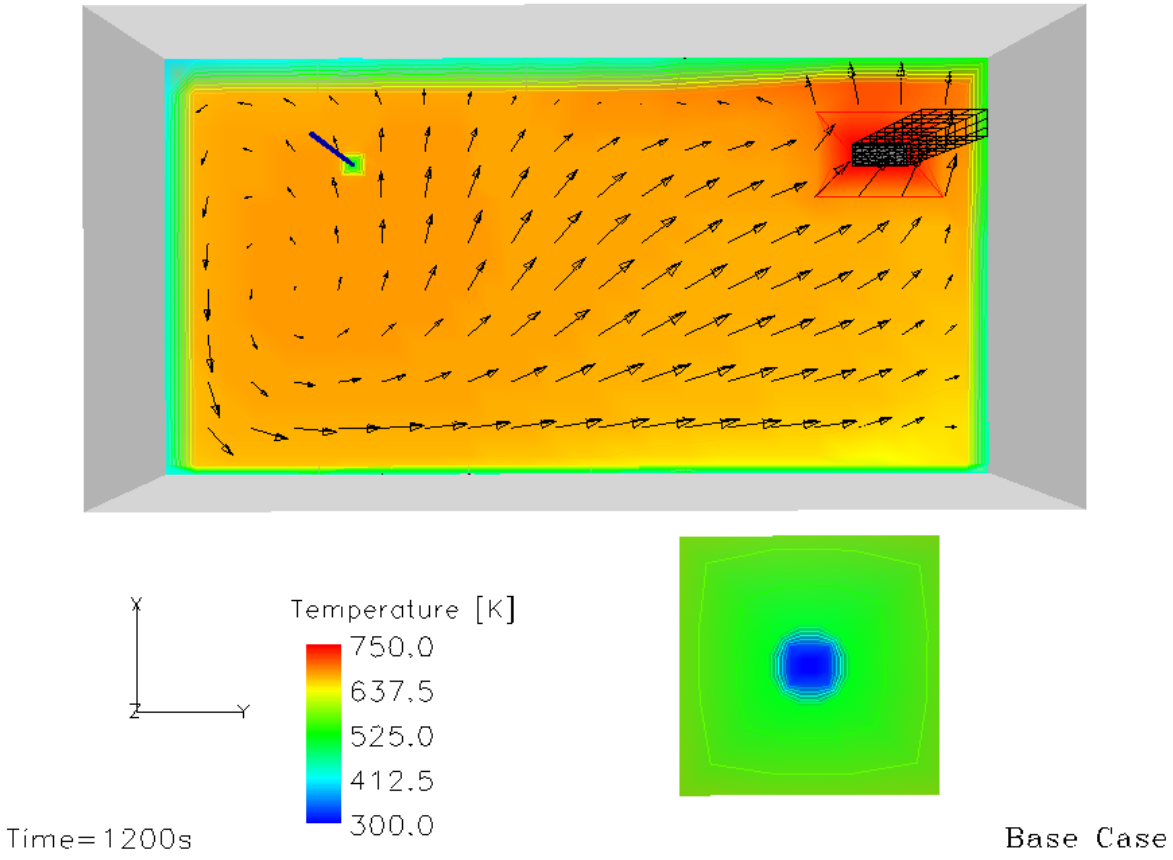

Fig. 17 Temperature distribution after 1200 s (base case)

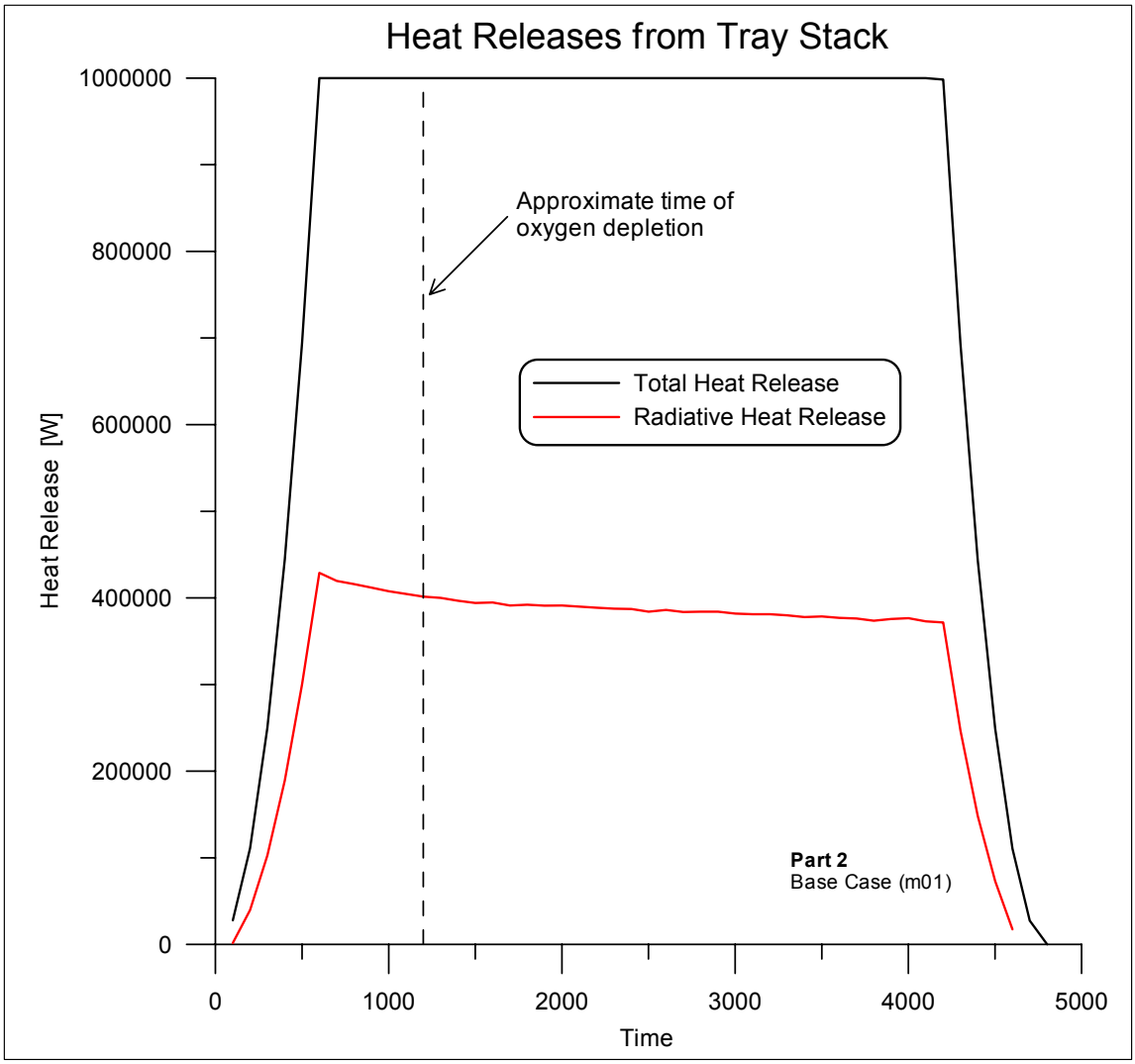

Fig. 18 Given heat release rate over time (part 2, base case)

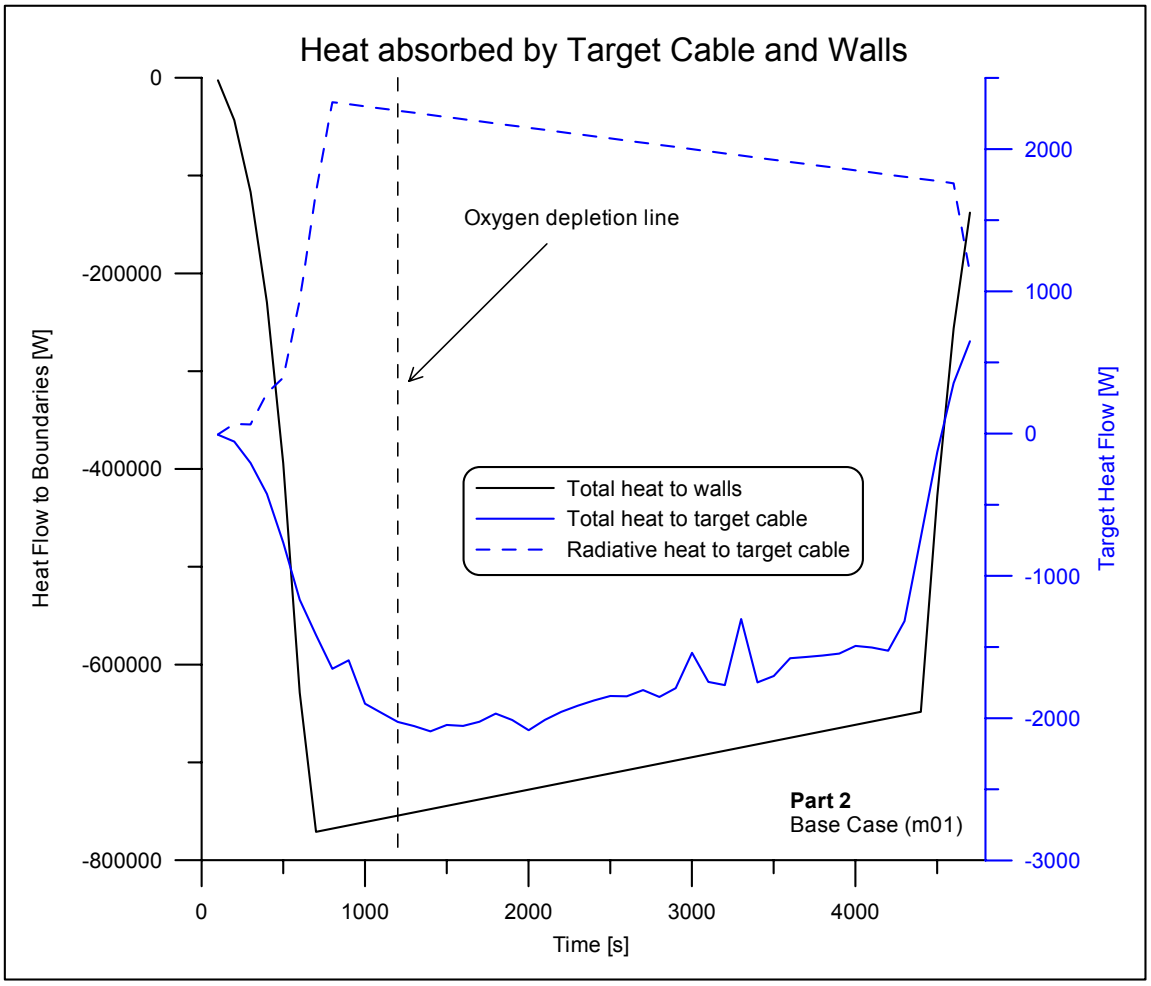

Fig. 19 Heat absorbed by the target cable (part 2, base case)

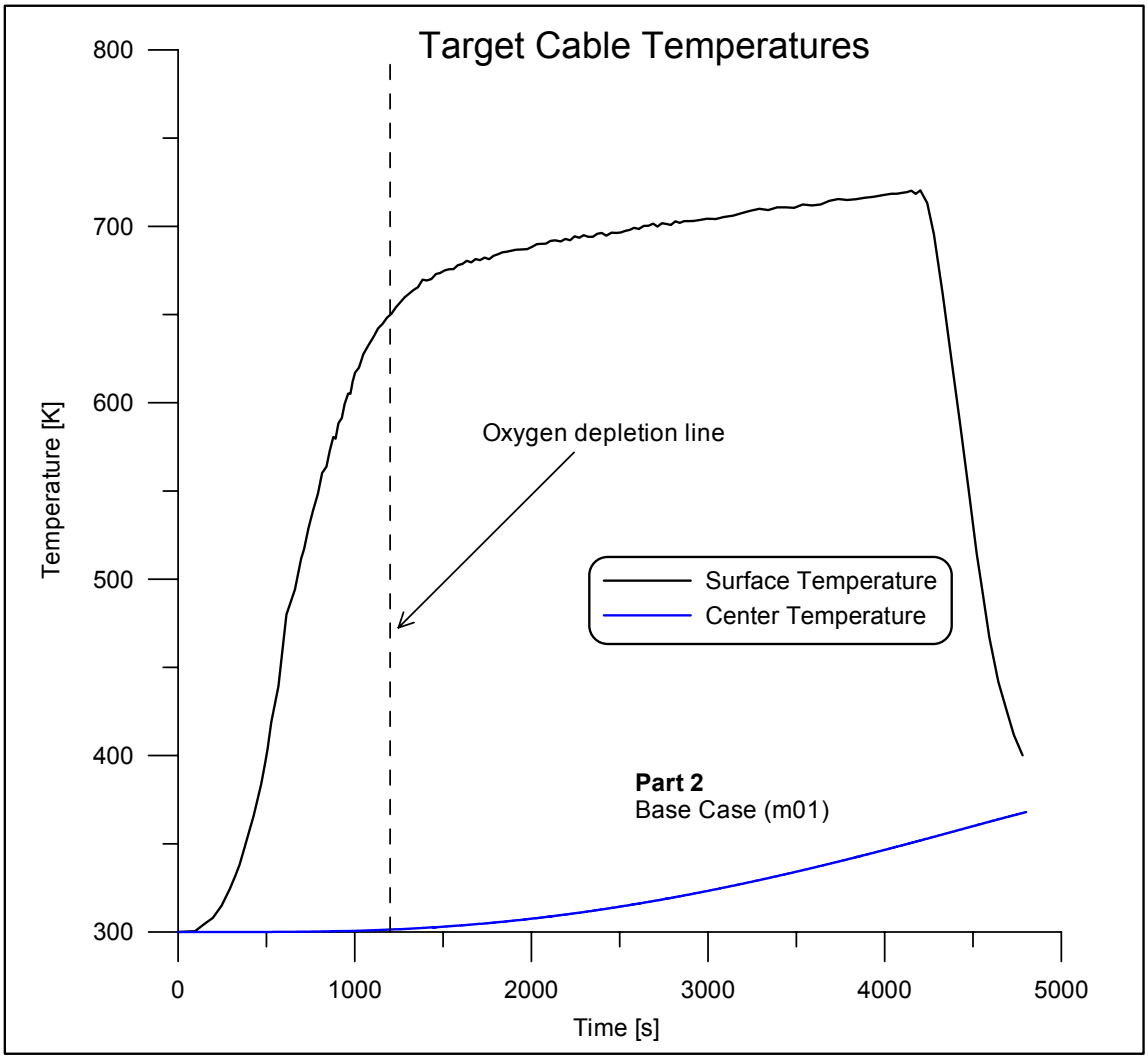

Fig. 20 Target cable temperatures during the base case of part 2

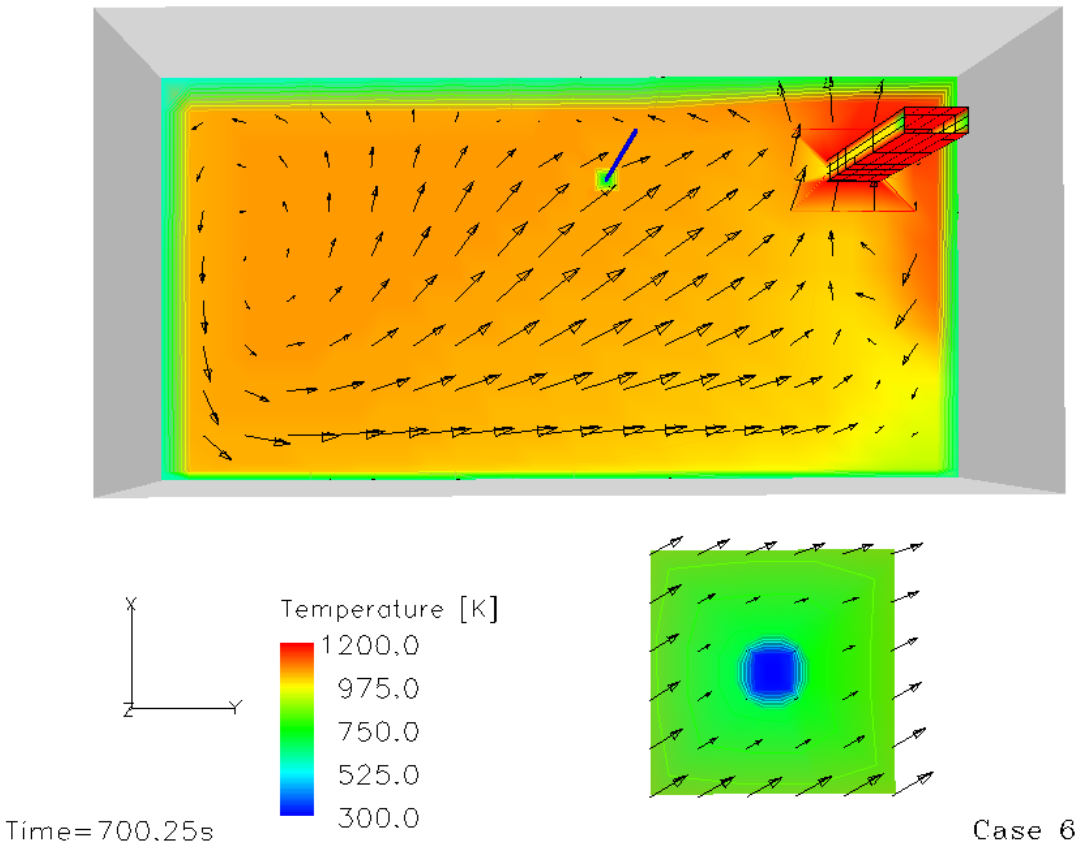

Fig. 21 Temperature distribution after 700 s for case 6

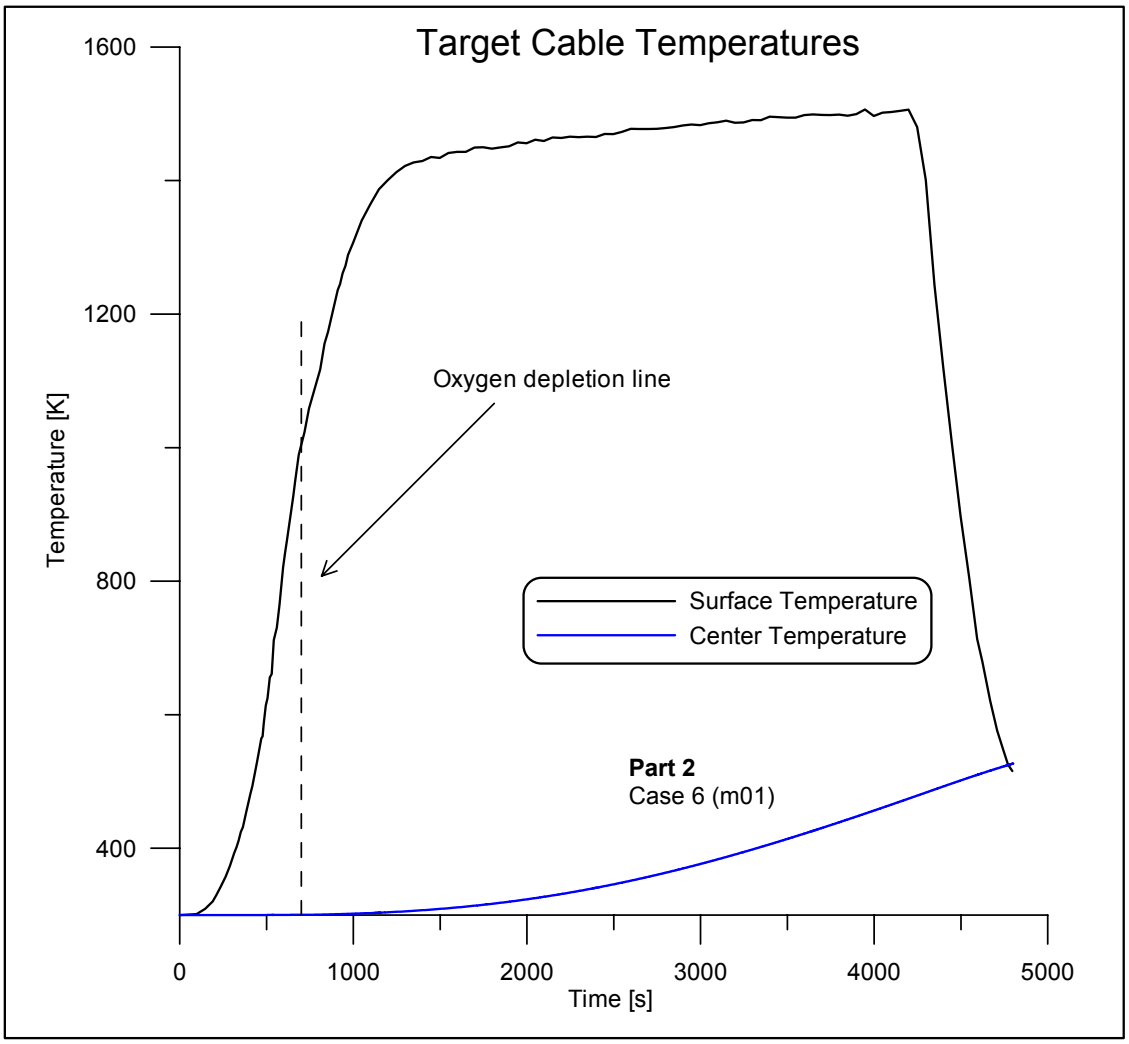

Fig. 22 Target cable temperatures for case 6

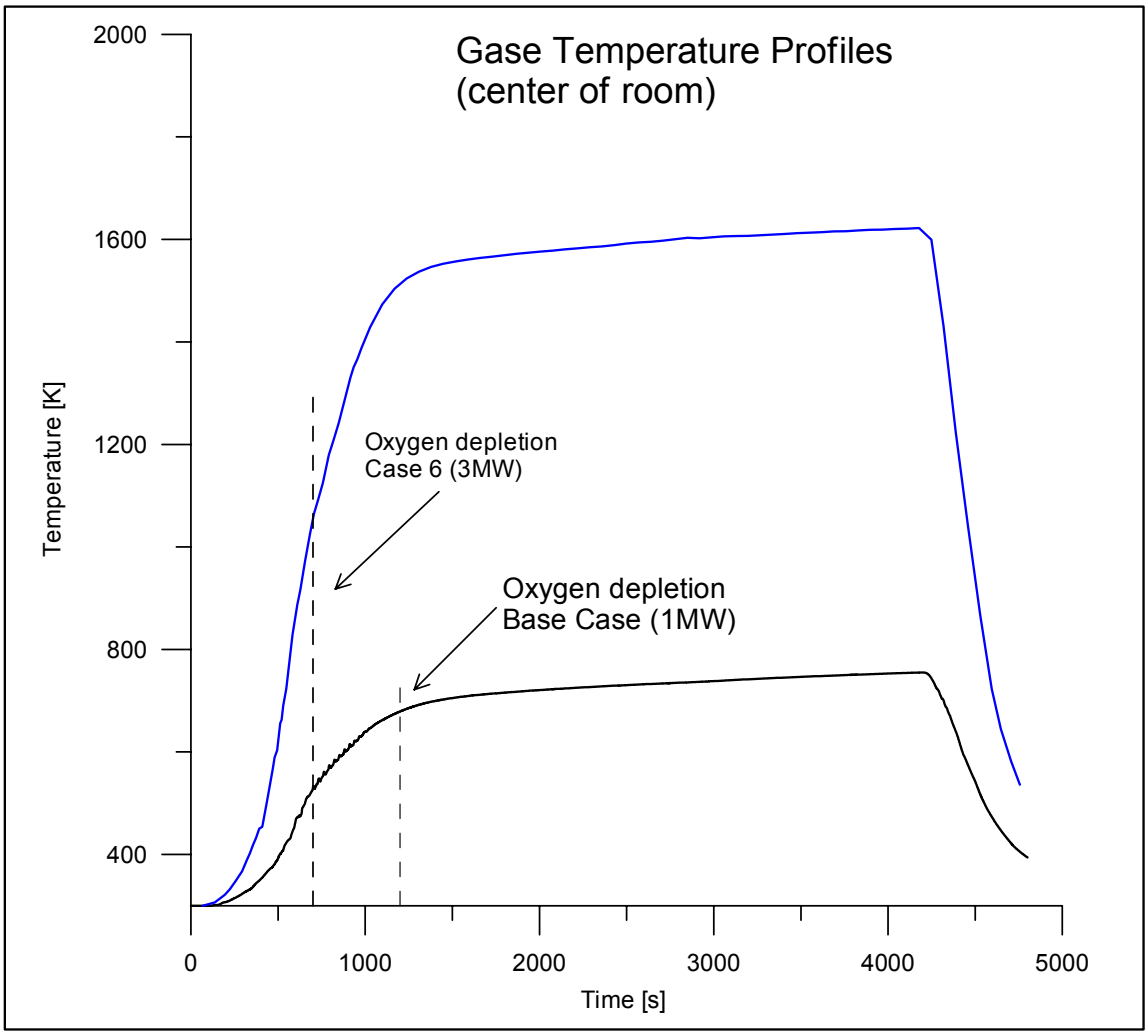

Fig. 23 Profile in the center of the room for base case and case 6

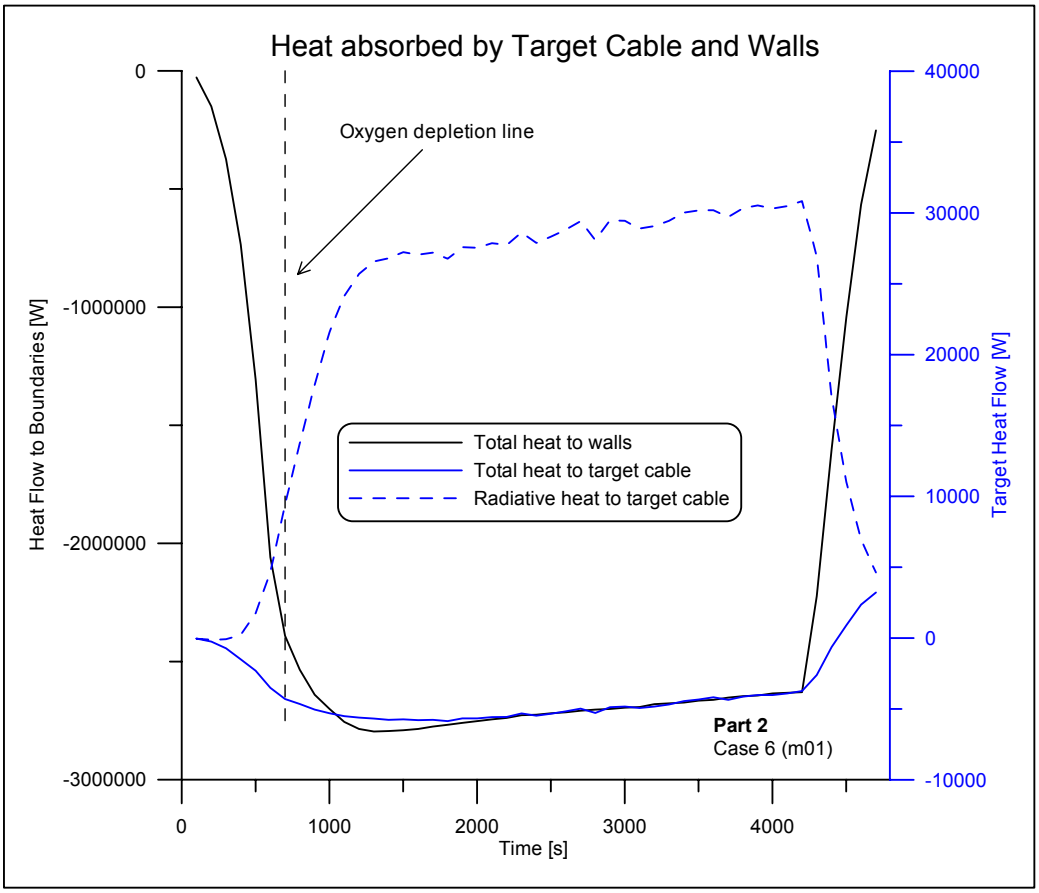

Fig. 24 Heat flows to walls and target cable for case 6

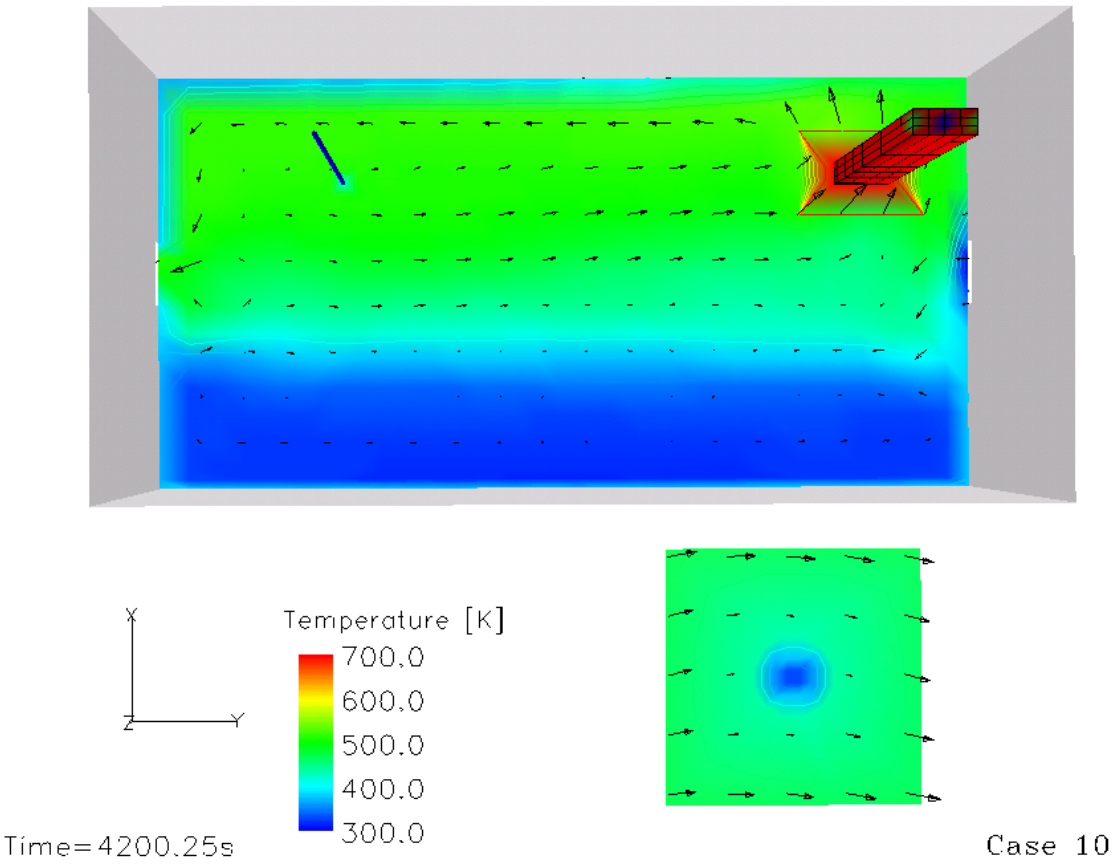

Fig. 25 Temperature stratification after 4200 s for case 10

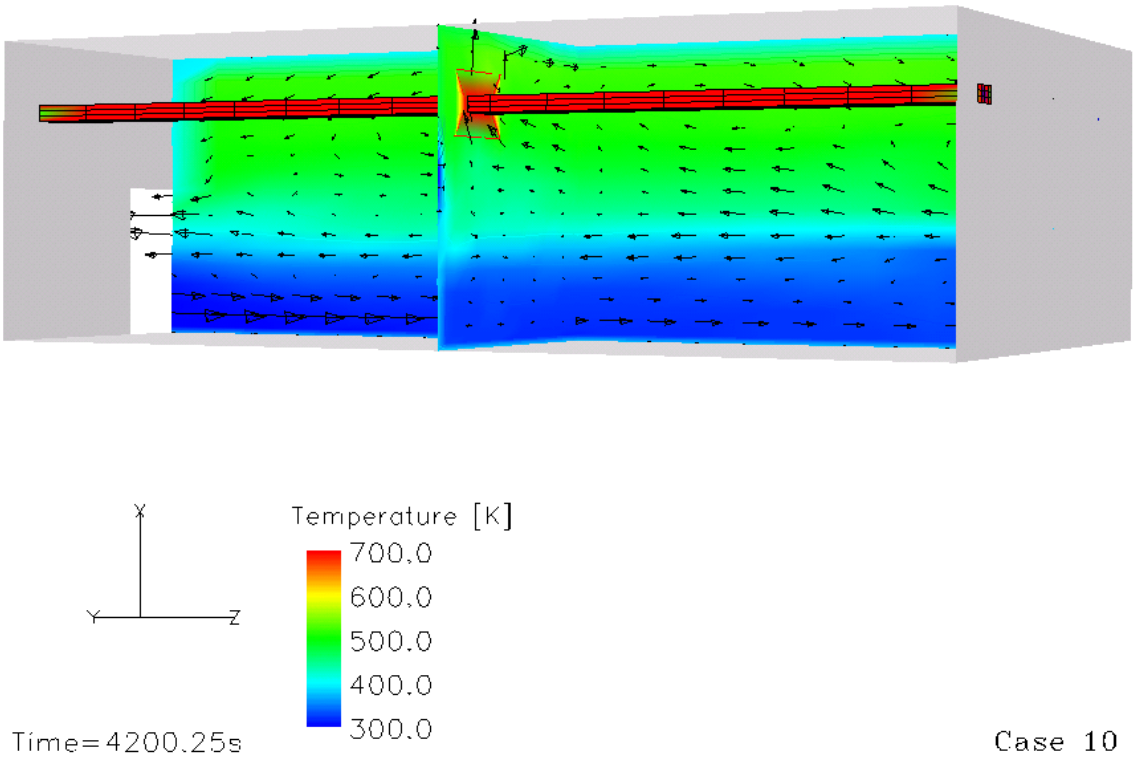

Fig. 26 Side view of the room at the end of the maximum power release

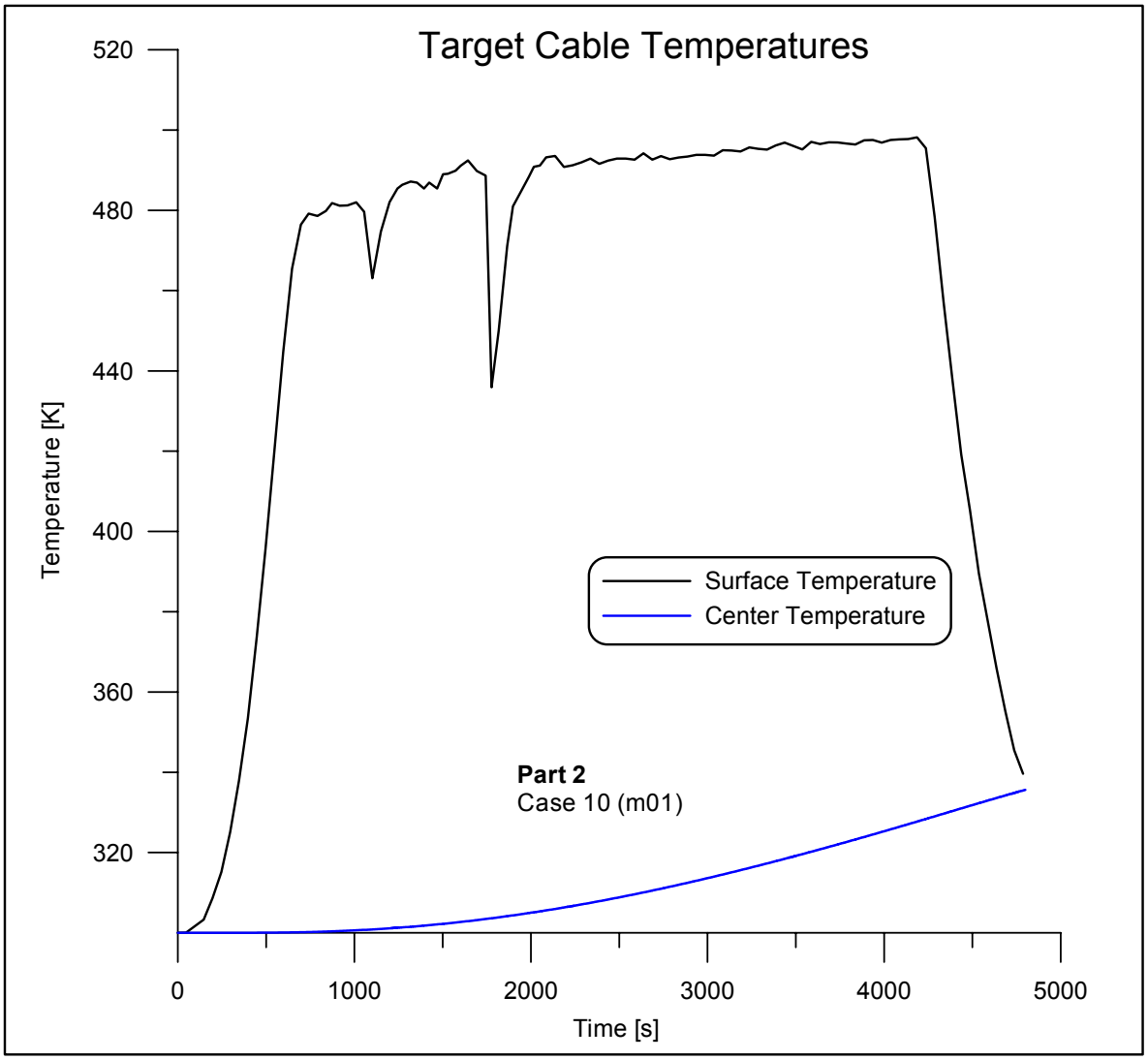

Fig. 27 Target temperatures over time for case 10

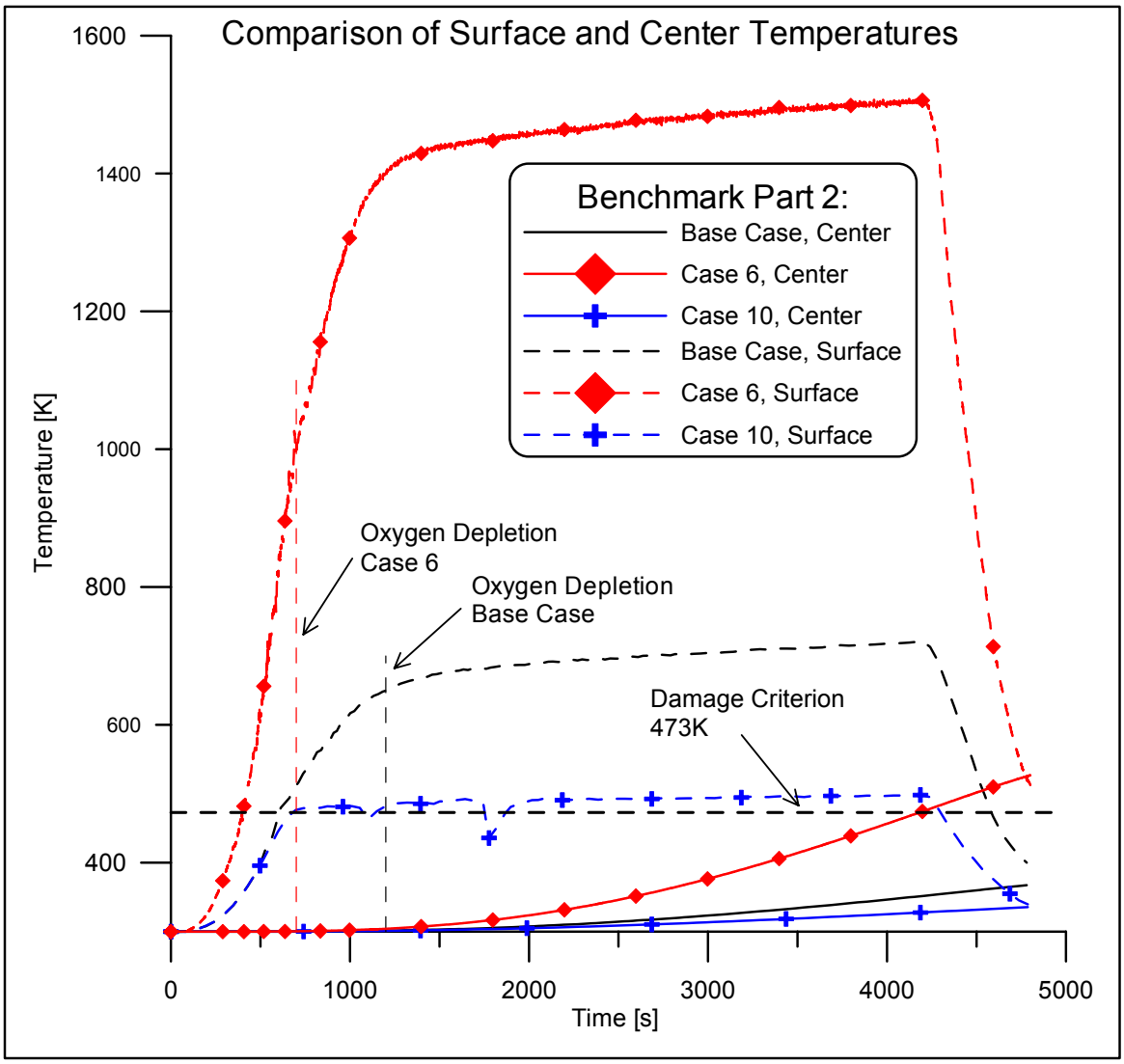

Fig. 28 Comparison of cable temperatures for base case, case 6 and case 10

Tab. 1 Summary of results of simulations

	Max. UL Temp. [K]	Max. Flux on Target [W/m^2]	Max. Target CL Temp [K]
Part 1			
Base Case	360 (180s)	210	300
Case 1	360 (180s)	210	300
Case 5	350 (180s)	210	300
Part 2			
Base Case	680 (1200s)	840	301 (368)
Case 6	1065 (700s)	5800 (700s)	532(4800s)
Case 10	525 (4200s)	500	335